Macromolecules
ARTICLE

Macromolecules **2009**, *42*, 6865–6872

DOI: 10.1021/ma901326h

Chiroptically Active Photonics Polymers: Synthesis and Chiroptically Switching Properties of Helical Polyacetylene Bearing Electrochromic Viologens in the Side Chains

Jian Deng, Can Zhou, and Naiheng Song*

Beijing National Laboratory for Molecular Sciences, Key Laboratory of Polymer Chemistry and Physics of Ministry of Education, College of Chemistry and Molecular Engineering, Peking University, Beijing 100871, China

Received June 19, 2009; Revised Manuscript Received August 14, 2009

ABSTRACT: Toward near-infrared chiroptically active photonics polymers, a new type of optically active polyacetylene bearing L-alanine and electrochromic viologen in the side chains was prepared and carefully studied for the chiroptical properties. The resulting polymer exhibited much larger optical rotation ($[m]^{25}{}_D = -1310°$, DMF) than the model compound ($[\varphi]^{25}{}_D = 201°$, DMF) as well as a strong negative circular dichroism (CD) signal attributable to backbone absorption, indicating the formation of a single-handed helical structure of the polymer main chain. The content of viologen in the polymer was determined to be > 70 mol % relative to the repeat unit by NMR and X-ray photoelectron spectrscopy. Because of the chiral perturbation of the helical main chain, the viologens in the side chains are asymmetrically positioned and interacted to yield a new strong negative CD band at long wavelengths (i.e., 450−800 nm) upon reduction to radical cations. The intensity of this CD signal could be easily switched between nearly 0 and -1.0×10^4 deg cm^2 dmol^{-1} by redox cycles, which could be repeated for five times without incurring any deterioration of the sample solution. The rotatory strength of the CD signal was calculated to be 1.3×10^{-40} esu^2 cm^2 according to Moffitt and Moscowitz's equation, which should contribute nontrivially to the chiroptical properties of the polymer at the near-infrared spectral region.

Introduction

Organic photonics polymers have been actively developed in the past 20 years because of their good structure−property tailorability and excellent processability, which allow for not only easy material optimization toward high performances but also great freedom in the design and fabrication of novel photonics devices.[1−7] However, most photonics polymers (e.g., waveguiding polymers,[4] nonlinear optical polymers,[5] and conjugated polymers[6,7]) that have been developed so far are linearly birefringent and make use of the interaction with light in the transverse electric (TE) and transverse magnetic (TM) modes; circularly birefringent photonics polymers capable of interacting with circularly polarized light are hardly known. Optically active polymers (i.e., polymers with chiral characteristics in the structure) are the unique types of materials that have inherent circular birefringence (or optical rotation, OR) and dichroism (CD) (i.e., the chiroptical properties). Such polymers have traditionally been developed for molecular recognition and asymmetric synthesis,[8] and their potential photonics applications have been underexplored to a great extent. Recently, studies have shown some important and niched photonics applications (e.g., nonlinear optics,[9] chirowaveguides,[10] left-handed metamaterials,[11] and optical switches[12]) for optically active materials; nevertheless, materials studies toward useful optically active polymers for photonics applications are still rare.

Chirowaveguide represents a straightforward photonics application for optically active polymers.[9] Different from conventional waveguiding materials, optically active polymers differentiate propagating light into right and left circularly polarized light rather than TE and TM waves. As a result, optically active polymers may be used as efficient polarization materials in their isotropic form, avoiding difficulties in the preparation of anisotropic structures required for conventional polarization materials (such as quartz and liquid crystals) as well as difficulties in the precise control of the polarization angle of incident light for anisotropic polarization materials. Furthermore, by the introduction of responsive groups to the optically active polymers,[12] controllable chiroptical properties under external fields (e.g., electric field and photo irradiation) may be achieved to allow for an active control of the polarization of light within the chirowaveguide, which is difficult to realize with anisotropic polarization materials but highly desirable for optical communication systems, especially for integrated optical systems.

For chirowaveguide applications, isotropic optically active polymers with very large and controllable chiroptical properties (e.g., $[\alpha]_\lambda > 1000°$) at application wavelengths, typically the near-infrared (NIR) telecommunication wavelengths at 1300−1500 nm, are highly desired. Although optically active materials showing large ORs in the UV−vis spectral region are known,[13,14] it appears challenging to develop optically active materials with large and controllable NIR chiroptical properties because of the optical rotatory dispersion and the lack of a control mechanism for chiroptical properties at the NIR spectral region. To overcome these challenges and toward optically active materials suitable for chirowaveguide applications, we have recently developed a structural model correlating the magnitude of chiroptical properties with the spatial arrangement of chromophores.[15] According to the model, a novel type of redox-driven chiroptical switching molecule having axially dissymmetric 1,1′-binaphthyl-2,2’-diyl as the chiral source and electrochromic viologen as the

---

*Corresponding author. E-mail: nsong@pku.edu.cn. Tel: +86-10-62755644.

chromophore was prepared to demonstrate the first example of chiral molecules exhibiting large and controllable NIR chiroptical properties {e.g., $[\theta]_{750\ \mathrm{nm}} = -8.44 \times 10^4$ deg cm^2 dmol^{-1} and $[\alpha]_{1500\ \mathrm{nm}} = -235°$}.[15,16] To further enhance the NIR chiroptical properties and to achieve materials with good thin-film processability, an optically active polymer with main-chain axial chirality and containing electrochromic viologens in the side chains was also prepared with the hope of taking advantage of the chiral amplification effect of the secondary chirality of the polymer main chain.[17] However, enhancement of chiroptical property of the polymer was only observed for OR in the UV−vis spectral region, and CD intensities attributable to reduced viologens were not increased, probably because of a weak interchromophoric interaction resulting from the low content (~50%) and unfavorable spatial arrangement of the viologens. Thus, to prepare highly efficient optically active polymers, it is desirable to position the low-band-gap chromophores in proximity and in a more favorable asymmetric environment, preferably with a macroscopic conformational chirality.

Single-handed helices are well-known secondary chiral structures capable of inducing very large chiroptical properties.[18] Optically active materials with such structures have been actively developed, and some of them (such as helicenes[13] and helical polymers[14,18]) exhibit extremely large specific ORs over 1000° at the sodium D line (i.e., 589 nm). Therefore, it can be expected that helical structures may also serve as an efficient structural motif for the induction of very large NIR chiroptical properties if low-band-gap chromophores can be introduced into the structure with appropriate asymmetric arrangements. On the basis of such a consideration, we have herein designed and synthesized a new type of optically active polymer by grafting the electrochromic viologens to the side chains of a single-handed helical polyacetylene. A high grafting ratio together with the chiral perturbation of the helical polymer main chain led to new CD signals because of asymmetrically arranged viologens, particularly in the absorption band (e.g., 450−800 nm) of reduced viologens (i.e., radical cations). The contribution of this new CD band to the OR of the polymer in the NIR spectral region was analyzed. Because of the good redox reversibility of viologens, a distinctive redox-driven chiroptically switching property was also revealed for the polymer at the absorption band of radical cations (e.g., $[\theta]_{530\ \mathrm{nm}}$ from nearly 0 to -1.0×10^4 deg cm^2 dmol^{-1}).

Experimental Section

Materials. 4-(Bromomethyl)benzoic acid,[19] 1-propyl-4-(4-pyridyl)pyridinium bromide (PPB; mp 188−189 °C),[20] 1-hexadecyl-4-(4-pyridyl)pyridinium bromide (HDPPB; mp 125−126 °C),[21] and $\mathrm{Rh^+(NBD)[B(C_6H_5)]_4}$[22] were prepared according to the literature methods. *N*,*N*′-Dimethylformamide (DMF) and acetonitrile (MeCN) were distilled over phosphorus pentoxide and calcium hydride, respectively, prior to use. All other chemicals and reagents were purchased from Beijing Chemical Reagent Company and used as received.

Measurements. NMR spectra were recorded at room temperature on either a Bruker ARX 400 MHz spectrometer (^{1}H NMR 400 MHz and ^{13}C NMR 100 MHz) or a Varian Mercury 300 MHz spectrometer (^{1}H NMR 300 MHz and ^{13}C NMR 75 MHz) using tetramethylsilane as an internal standard. The chemical shifts are reported in the ppm scale. Gel permeation chromatographic (GPC) measurements were performed with a Waters 2410 refractive index detector at room temperature. Tetrahydrofuran (THF) was used as the eluent with a flow rate of 1.0 mL/min. All GPC data were calibrated with linear polystyrene standards. IR spectra were recorded on a Nicolet Magna 750 Fourier transform infrared (FT-IR) spectrometer. Electrospray ionization mass spectrometry (ESI-MS) spectra were measured on a Bruker HCT Ultra ESI-MS mass spectrometer. Elemental analysis was conducted by an Elementar Vario EL instrument (Elementar Analysensysteme GmbH). X-ray photoelectron spectroscopy (XPS) data were taken on an AXIS-Ultra instrument from Kratos Analytical using monochromatc Al Kα radiation (225 W, 15 mA, 15 kV) and low-energy electron flooding for charge compensation. The binding energies were calibrated using a C 1s hydrocarbon peak at 284.80 eV. The data were converted into VAMAS file format and imported into a *CasaXPS* software package for manipulation and curve-fitting. UV−vis absorption spectra were recorded with a Varian Cary 1E spectrometer. ORs were measured at 25 °C using a Jasco model P-1030 polarimeter. CD spectra were recorded on a Jasco J-810 spectropolarimeter. Thermogravimetric analysis (TGA) was performed on a TA Q600 instrument at a heating rate of 10 °C/min in nitrogen. Differential scanning calorimetry (DSC) was recorded with a Perkin-Elmer Pyris I differential scanning calorimeter in nitrogen.

Cyclic voltammetry (CV) was conducted using a CHI 600C voltammetric analyzer. The experiments were performed at room temperature in DMF solutions containing 0.1 M tetrabutylammonium perchlorate ($\mathrm{Bu_4NClO_4}$) as the supporting electrolyte at a scan speed of 100 mV/s. A conventional three-electrode cell consisting of a glassy carbon disk (diameter 2 mm, freshly polished) as the working electrode, a platinum stick (1 mm thick) as the counter electrode, and AgCl/Ag as the reference electrode was used. All potentials reported here are potentials measured versus the AgCl/Ag electrode.

Redox-based spectroscopic measurements were made chemically by using an OTTLE-type quartz cell with an optical path length of 1 mm and in nitrogen-saturated DMF. A soldering-tin-attached platinum grid of size 6 × 20 mm^2 and 800 mesh/cm^2 was used as the reducing agent. During experiments, the soldering tin together with the platinum grid was immersed into the solution, and reduction occurred on the surfaces of both the tin particle and the platinum grid. Oxidation of reduced sample solutions was readily done by shaking of the cell in air.

Synthesis of Monomers. *N-tert-Butoxycarbonyl-L-alanine Propargylamide* (***1***). The synthesis of **1** is referred to the literature method[23] and modified as follows: To an ice-cold, nitrogen-protected solution of dicyclohexylcarbodiimide (9.60 g, 46.5 mmol) and *N-tert*-butoxycarbonyl-L-alanine (8.00 g, 42.3 mmol) in THF (180 mL) was added propargylamine (2.96 mL, 2.60 g, 46.5 mmol) and 4-(dimethylamino)phenol (0.06 g, 0.48 mmol). The resulting solution was allowed to warm slowly to room temperature and stirred for 12 h. The solution was filtered, and the filtrate was rotaevaporated to give a light-yellow solid product that was recrystallized from ethyl acetate to yield white crystals (4.50 g, 72% yield): mp 145−146 °C; $[\alpha]^{25}_{\mathrm{D}} = -34.0°$ (0.4, $\mathrm{CHCl_3}$); ^{1}H NMR (400 MHz, $\mathrm{CDCl_3}$) δ 6.52 (1H, br s), 4.98 (1H, br s), 4.18 (1H, br s), 4.05 (2H, br s), 2.23 (1H, t, J = 2.6 Hz, 2.6 Hz), 1.49 (9H, s), 1.37 (3H, d, J = 7.2 Hz).

N-4-(Bromomethyl)benzoyl)-L-alanine Propargylamide (**2**). A mixture solution of 4-(bromomethyl)benzoic acid (1.50 g, 6.98 mmol) in thionyl chloride (5 mL) was stirred at reflux for 3 h. The excess amount of thionyl chloride was removed under vacuum (1 mmHg) to yield 4-(bromomethyl)benzoyl chloride as a white solid, which was used for the following synthesis without further purification.

A mixture solution of **1** (1.60 g, 7.07 mmol) in hydrochloric acid (3 M, 24 mL) was stirred at room temperature for 4 h. The solution was filtered to remove any insoluble particles. To the filtrate was added distilled water (30 mL) and powdered potassium carbonate to adjust the pH value to 8. To the resulting solution was slowly added the above freshly prepared 4-(bromomethyl)benzoyl chloride in chloroform (100 mL). The mixture solution was stirred at room temperature for 3 h. Powdered potassium carbonate was added during the course of reaction to maintain the pH in the range of 8−9. Ethyl acetate was added to the mixture to dissolve the resulting white precipitate. The organic phase was separated and rotaevaporated to remove most of the solvent. The aqueous phase was washed in a separatory funnel with ethyl acetate (4 × 50 mL). The organic phases were combined, washed in sequence with an aqueous sodium carbonate solution (2 M, 2 × 30 mL), hydrochloric acid (3 M, 2 × 30 mL), and distilled water (2 × 30 mL), and dried over anhydrous magnesium sulfate. After the solvent was removed by rotaevaporation, the resulting white powdered product was recrystallized from ethyl acetate to yield white needlelike crystals (1.30 g, 58% yield): mp 168−169 °C; $[\alpha]^{25}{}_{D} = +5.6°$ (0.40, $CHCl_3$), +71.5° (0.40, DMF); ^1H NMR (400 MHz,$CDCl_3$) δ 7.78 (2H, d, $J = 8.0$ Hz), 7.45 (2H, d, $J = 8.0$ Hz), 6.93 (1H, br s), 6.83 (1H, br s), 4.78−4.74 (1H, m), 4.50 (2H, s), 4.07−4.11 (2H, m), 2.23 (1H, t, $J = 2.4$ and 2.4 Hz), 1.52 (3H, d, $J = 6.9$ Hz); ^{13}C NMR (75 MHz, $CDCl_3$) δ 171.9, 166.6, 141.7, 133.4, 129.2, 127.7, 79.1, 71.8, 49.1, 32.1, 29.3, 18.4; FT-IR (KBr, cm^{-1}): 3290.5, 3062.9, 2929.8, 1629.8, 1537.2, 1334.7, 1240.2, 696.3; ESI-MS (m/z) 671, 669, 667 ($[2M+Na]^+$), 347, 345 ($[M+Na]^+$), 325, 323 ($[M+H]^+$). Anal. Calcd for $C_{14}H_{15}BrN_2O_2$: C, 52.03; H, 4.68; N, 8.67. Found: C, 51.99; H, 4.83; N, 8.61.

N-[4-(1′-Propyl-4,4′-bipyrid-1-yl)methylbenzoyl]-L-alanine Propargylamide (***3***). A solution of **2** (0.30 g, 0.93 mmol) and PPB (0.30 g, 1.07 mmol) in methanol (10 mL) was stirred under nitrogen at 50 °C for 17 h. After cooling to room temperature, the solution was removed by a rotaevaporator. The residue was washed thoroughly with hot chloroform and dried overnight in a vacuum oven at 60 °C (1.51 g, 91% yield): $[\alpha]^{25}{}_{D} = +33.5°$ (0.40, DMF); ^1H NMR (400 MHz, DMSO-d_6) δ 9.52 (2H, d, $J = 6.5$ Hz), 9.38 (2H, d, $J = 6.5$ Hz), 8.79 (2H, d, $J = 6.7$ Hz), 8.77 (2H, d, $J = 6.5$ Hz), 8.58 (1H, d, $J = 7.8$ Hz), 8.41 (1H, t, $J = 7.2$ and 7.2 Hz), 7.99 (2H, d, $J = 8.1$ Hz), 7.69 (2H, d, $J = 8.2$ Hz), 6.01 (2H, s), 4.66 (2H, t, $J = 7.3$ and 7.3 Hz), 4.44−4.48 (1H, m), 3.85−3.86 (2H, m), 3.12 (1H, t, $J = 3.2$ and 3.2 Hz), 1.99−2.01 (2H, m), 1.31 (3H, d, $J = 7.2$ Hz), 0.92 (3H, t, $J = 7.4$ and 7.3 Hz); ^{13}C NMR (75 MHz, DMSO-d_6) δ 172.1, 165.3, 149.2, 148.5, 145.9, 145.7, 137.1, 134.9, 128.8, 128.4, 127.2, 126.7, 81.3, 73.0, 62.7, 62.1, 48.9, 28.0, 24.2, 17.9, 10.2; FT-IR (KBr, cm^{-1}) 3391.5, 3282.6, 3044.4, 1644.2, 1534.2, 1446.5, 1248.8, 806.2; ESI-MS (m/z) 442 ($[M]^+$), 441 ($[M-H]^+$), 221 ($[M]^{2+}$).

N-[4-(1′-Hexadecyl-4,4′-bipyrid-1-yl)methylbenzoyl]-L-alanine Propargylamide (***4***). A 25 mL round-bottomed flask was charged with **2** (0.15 g, 0.47 mmol), HDPPB (0.20 g, 0.44 mmol), and MeCN (6 mL). The solution was refluxed under nitrogen for 8 h. After cooling to room temperature, the resulting mixture solution was filtered to collect the yellow solid product, which was thoroughly washed with MeCN and acetone and dried at 60 °C under vacuum (0.25 g, 71% yield): $[\alpha]^{25}{}_{D} = +8.5°$ (0.4, MeOH); ^1H NMR (400 MHz, DMSO-d_6) δ 9.58 (2H, d, $J = 6.5$ Hz), 9.43 (2H, d, $J = 6.5$ Hz), 8.84 (2H, d, $J = 6.5$ Hz), 8.80 (2H, d, $J = 6.5$ Hz), 8.59 (1H, d, $J = 7.8$ Hz), 8.40 (1H, t, $J = 5.6$ and 5.6 Hz), 7.98 (2H, d, $J = 8.0$ Hz), 7.72 (2H, d, $J = 8.0$ Hz), 6.05 (2H, s), 4.70 (2H, t, $J = 7.2$ and 7.2 Hz), 4.44−4.48 (1H, m), 3.84−3.86 (2H, m), 3.11 (1H, s), 1.97 (2H, br s), 1.23−1.33 (29H, m), 0.85 (3H, t, $J = 6.4$ Hz); ^{13}C NMR(100 MHz, DMSO-d_6) δ 171.9, 165.2, 149.2, 148.5, 145.8, 145.7, 136.9, 134.9, 128.7, 128.3, 127.1, 126.7, 81.0, 72.9, 62.8, 60.8, 48.8, 31.2, 30.7, 29.0, 28.98, 28.96, 28.91, 28.8, 28.6, 28.4, 27.9; ESI-MS (m/z): 705.3 ($[M-Br]$), 623.6 ($[M-2Br-H]^+$), 381.4 ($[M_{HDPPB}-Br]$).

Polymer Synthesis. *Polymerization of Monomer 2 [Poly(2)].* A number of polymerization conditions of **2** were studied, and a preferred reaction condition is described as follows: To a solution of **2** (0.26 g, 0.80 mmol) in degassed THF (8 mL) was added $Rh^+(NBD)[B(C_6H_5)]^4$ (4.0 mg, 8.0 μmol). The resulting mixture was stirred vigorously at 0 °C for 24 h under nitrogen before being poured into ligroin (150 mL) to precipitate the polymer. The resulting solid product was collected by vacuum filtration through a poly(tetrafluoroethylene) (PTFE) membrane filter (pore size 0.45 μm), washed thoroughly with methanol, and vacuum-dried at 60 °C overnight (0.13 g, 51% yield): $M_n = 7.5 \times 10^3$ (PDI = 1.85, GPC); $[\alpha]^{25}{}_{D} = -123°$ (0.4, $CHCl_3$), $[\alpha]^{25}{}_{D} = -139°$ (0.4, THF); FT-IR (KBr, cm^{-1}): 3299.0, 1643.2, 1529.4, 1230.5; T_g = not detectable (DSC, N_2); $T_{d,5\%} = 206$ °C (TGA, N_2).

Grafting of HDPPB onto Poly(2) [Poly(4)]. A solution of poly(**2**) (0.060 g, 0.18 mmol) and HDPPB (0.171 g, 0.372 mmol) in methanol (20 mL) was stirred at room temperature for 24 h under nitrogen. The solution was concentrated to ~5 mL by rotaevaporation before being poured into MeCN (200 mL) to precipitate the polymer. The resulting solid product was collected by filtration through a PTFE membrane filter (pore size 0.45 μm), thoroughly washed with MeCN and acetone, and dried overnight in a vacuum oven at 60 °C (0.098 g, 67% yield): $[\alpha]^{25}{}_{D} = -167°$ (0.40, DMF), $[\alpha]^{25}{}_{D} = -71°$ (0.40, MeOH); FT-IR (KBr, cm^{-1}) 3411.8, 2923.8, 2852.5, 1638.4, 1533.3, 1500.5, 1447.5, 1271.9, 1169.7; T_g = not detectable (DSC, N_2); $T_{d,5\%} = 213$ °C (TGA, N_2).

Results and Discussion

Synthesis. To obtain single-handed helical polyacetylenes bearing electrochromic viologen groups in the side chains, viologen-containing chiral acetylene monomer **3** was initially designed and synthesized via a three-step reaction route (Scheme 1). However, direct polymerizations of **3** by using rhodium-based catalysts {e.g., $[Rh(nbd)Cl]_2$, $(nbd)Rh^+[B(C_6H_5)]_4^-$, and $Rh(cod)(tos)(H_2O)$} failed to produce high-M_w polymers (e.g., $M_n < 2.0 \times 10^3$ or degree of polymerization (DP) < 4, as determined by water-phase GPC), and the resulting oligomers exhibited poor solubility in common organic solvents (e.g., MeCN, chloroform, and DMF) and small ORs (e.g., $[\alpha]_D < 40°$). In order to overcome this problem and to achieve high-M_w polyacetylenes, we thus carried out the rhodium-catalyzed polymerization of monomer **2** using $(nbd)Rh^+[B(C_6H_5)]_4^-$ as the catalyst to prepare the benzyl bromide-containing poly(**2**), followed by grafting of PPB through a quarternization reaction. Poly(**2**) was obtained at a yield of ca. 50% and with a moderate number-average molecular weight [$M_n = (7.5-8.3) \times 10^3$ or DP = 23−26, as determined by GPC in THF] and large ORs ($[\alpha]_D$ = −115 to −132°). However, the subsequent grafting of PPB to poly(**2**) again proved to be unsuccessful because of early precipitation of poly(**3**) from a solution such as MeCN, methanol, or DMF (Scheme 1). Therefore, HDPPB that has a long alkyl substituent was prepared and grafted onto poly(**2**) to give the viologen-containing polyacetylene poly(**4**) (Scheme 1). In contrast to poly(**3**), poly(**4**) exhibited good solubility in polar organic solvents such as methanol and DMF and can be readily prepared in uniform thin films by a spin-coating technique. No degradation of the polyacetylene main chain was found during the grafting reaction, as evidenced by GPC measurements, which revealed no decrease in the molecular weight for poly(**2**) after being subjected to the same grafting reaction conditions for 24 h. For comparison purposes, viologen-containing acetylene **4** was also prepared as a model compound for poly(**4**) (Scheme 1).

The structures of poly(**2**) and poly(**4**) were examined by NMR, IR, and XPS. Figure 1 shows the ^1H NMR spectra of the polymers. Peaks associated with aromatic viologen protons are clearly observable for poly(**4**), indicating the successful grafting of HDPPB. On the basis of the integrated peak ratio (0.52) between aromatic viologen protons and all of the aromatic and amide protons at $\delta > 7.0$ ppm, a HDPPB grafting ratio of 80% was estimated. Both poly(**2**) and poly(**4**) exhibited broad resonance peaks at around 6.05 ppm, attributable to the cis vinyl protons of the main chain. By calculation of the integration ratio of the cis vinyl protons relative to all of the aromatic and amide protons at $\delta > 6$ ppm, a cis content of 57% was estimated for poly(**2**). For poly(**4**), the cis content was not calculated because of the overlap

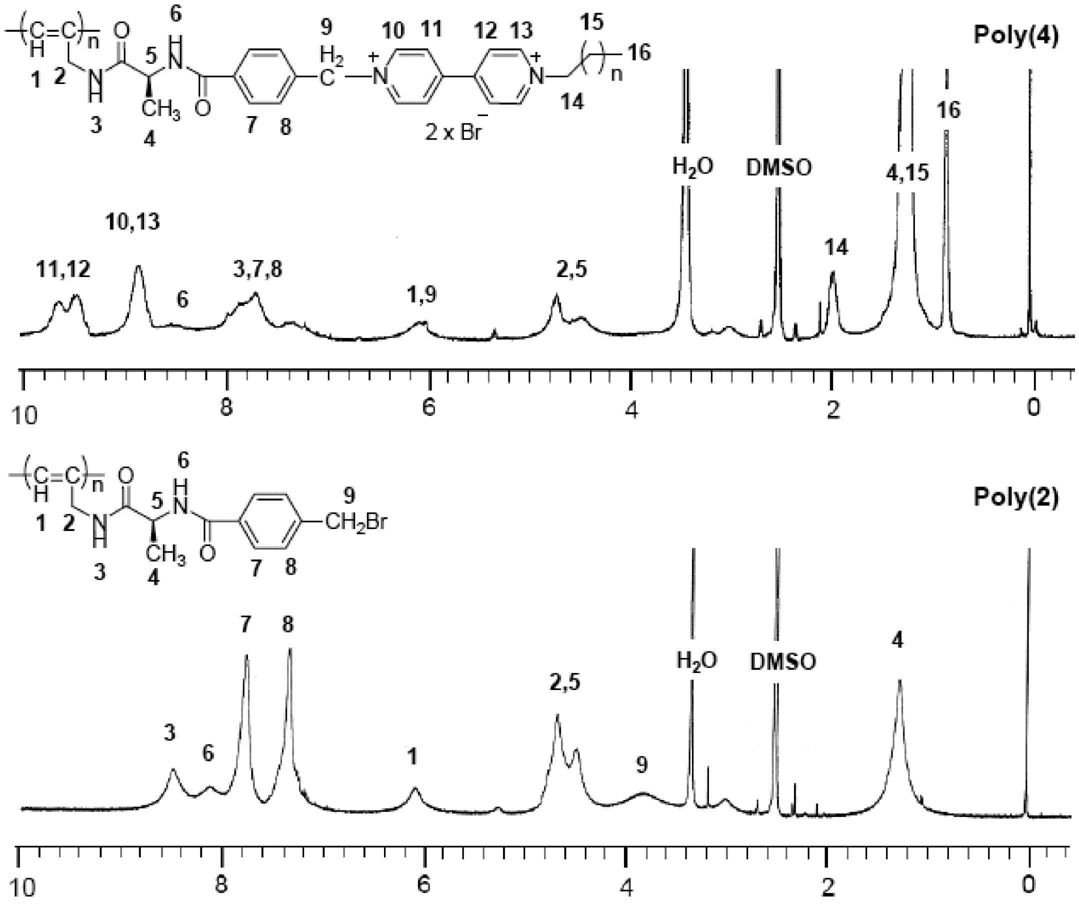

Figure 1. ^{1}H NMR spectra of poly(**2**) and poly(**4**) in DMSO-d_6.

Scheme 1. Synthesis of Helical Polyacetylene Bearing Viologens in the Side Chains

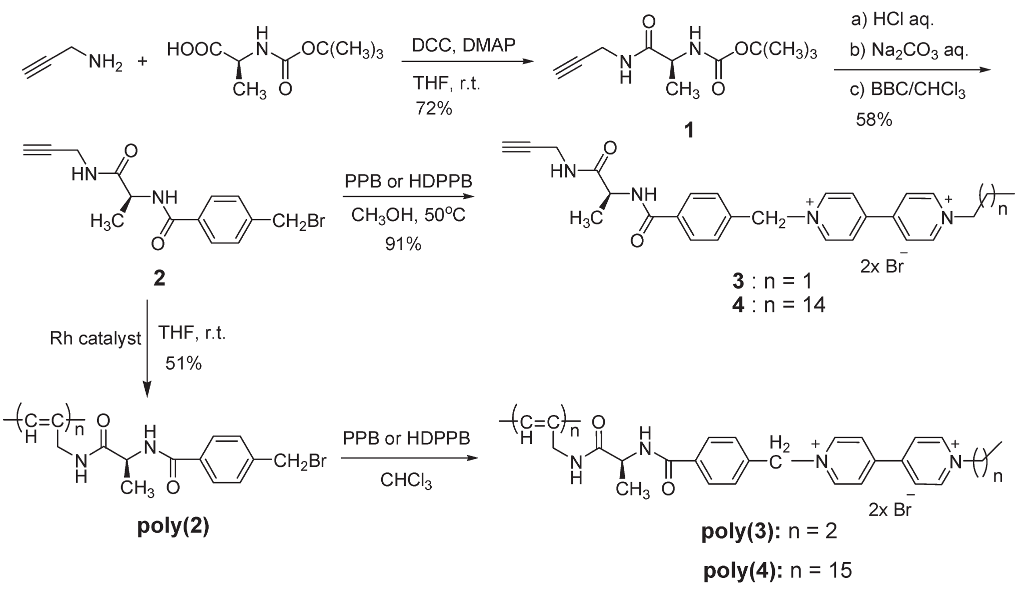

between the resonant peaks of the vinyl proton H-1 and the methylene proton H-9 (Figure 1). However, similar cis contents can be expected for poly(**2**) and poly(**4**) because of the mild grafting reaction conditions.

To further confirm the viologen content in the polymer, XPS spectra of poly(**2**) and poly(**4**) were recorded. Figure 2 shows the XPS wide-scan and C 1s, N 1s, and Br 3d core-level spectra. For poly(**2**), the N 1s core-level spectrum is fitted with one peak at 399.8 eV, attributable to the amide nitrogen atoms, while the Br 3d core-level spectrum can be deconvoluted into a spin−orbit doublet with the binding energies for Br 3d$_{5/2}$ and Br 3d$_{3/2}$ component peaks at 70.0 and 71.1 eV, respectively, corresponding to the chemically bonded bromine (Br) of benzyl bromide. In contrast, the N 1s core-level spectrum of poly(**4**) can be fitted with two peaks at 399.7 and 402.1 eV, with the latter peak attributable to the cationic

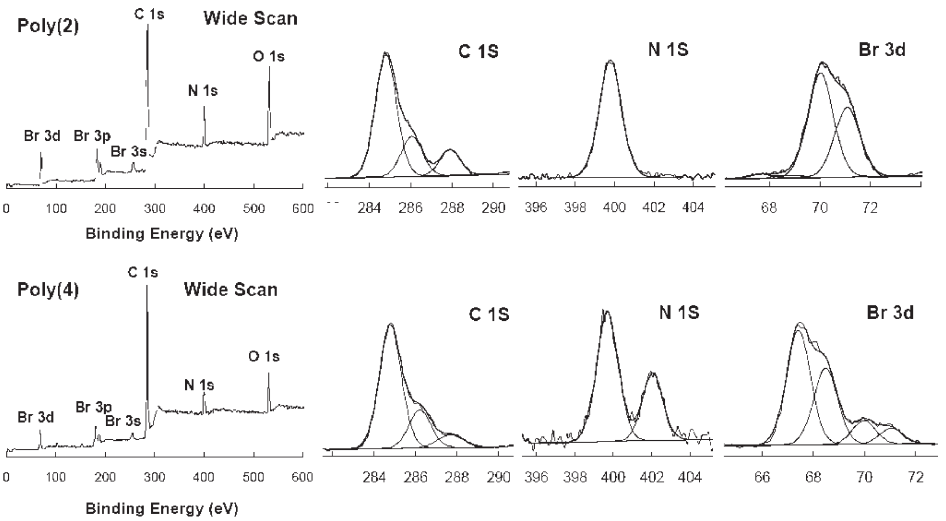

Figure 2. XPS wide-scan and core-level (C 1s, N 1s, and Br 3d) spectra of poly(**2**) and poly(**4**).

nitrogen (N^+) of the viologen unit. Given that a viologen radical cation ($V^{\bullet+}$) can readily form during X-ray excitation and the radical-cation nitrogen ($N^{\bullet+}$) has a binding energy of ca. 399.7 eV,[24] the peak at 399.7 eV for poly(**4**) should be assignable to the mixture of amide nitrogen and $N^{\bullet+}$. On the basis of the N/C ratio (0.1) calculated from the XPS analysis, a viologen grafting ratio of 100% is estimated. The Br 3d core-level spectrum of poly(**4**) can be deconvoluted into two spin–orbit doublets with binding energies of 67.4 and 68.5 eV for the first doublet, attributable to the Br $3d_{5/2}$ and Br $3d_{3/2}$ of the ionic bromine (Br^-), and binding energies of 70.0 and 71.0 eV for the second doublet, attributable to the chemically bonded Br. On the basis of the area ratio of Br^-/Br, a viologen grafting ratio of 71% is estimated. Thus, according to the above NMR and XPS analysis results, a viologen grafting ratio of more than 70% can be concluded. At such a high grafting ratio (i.e., more than two viologen groups on every three repeat units), the viologen chromophores in the side chains are expected to be able to interact closely and contribute to the chiroptical properties.

The thermal stabilities of poly(**2**) and poly(**4**) were examined by TGA in nitrogen. Both polymers showed on-set temperatures for weight loss (T_d) at ca. 200 °C, corresponding to decomposition of the viologen groups and the polyacetylene main chain. No glass transition temperature was detected by DSC before 200 °C.

Chiroptical Properties. Poly(*N*-propargylamide) bearing chiral units in the side chains is known to form helical structures with single-handed screw sense.[25,26] Intermolecular hydrogen bonding between amide groups plays an important role in such a secondary structure. In our study, both poly(**2**) and poly(**4**) show much larger absolute specific rotations than their corresponding monomers. This is also true when mean-residue molar ORs per repeat unit ($[m]_D^T$, deg cm^2 mol^{-1}) of poly(**2**) and poly(**4**) are taken into account. As shown in Figure 3, the $[m]_D$'s of poly(**2**) in chloroform and poly(**4**) in DMF are −397° and −1310°, respectively, much larger than the molar ORs ($[\phi]_D$) of **2** (+18°, $CHCl_3$) and **4** (+201°, DMF), suggesting the formation of a single-handed helical conformation of the main chain. Masuda et al.[26] reported a solvent effect on the chiroptical properties of poly(*N*-propargylamide) due to a different hydrogen-bonding mechanism and chain conformation in different solvents. A similar solvent effect was also observed in our study. As shown in Figure 3, poly(**2**) exhibited a larger $[m]_D$ in THF (−449°) than in chloroform, and poly(**4**) showed a much smaller $[m]_D$ in methanol (−777) than in DMF.

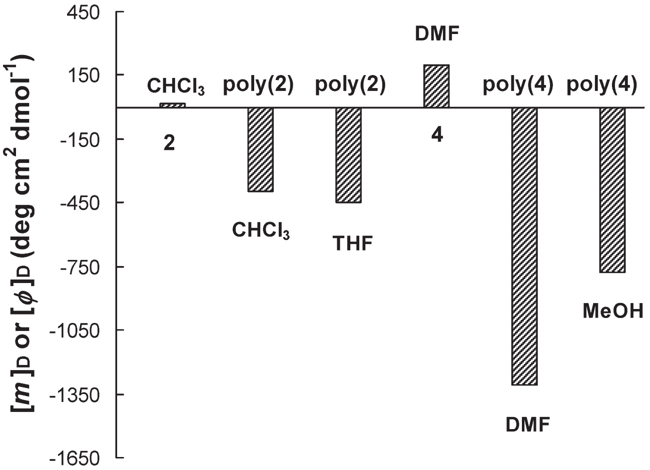

Figure 3. Comparison of molar ORs of **2** and **4** and mean-residue molar ORs per repeat unit of poly(**2**) and poly(**4**) in different solvents.

Figure 4 depicts the UV–vis and CD spectra of poly(**2**), poly(**4**), and **4**. Both poly(**2**) and poly(**4**) exhibit a shoulder absorption at around 330 nm, attributable to the conjugated polyacetylene main chain. In comparison, poly(**4**) in methanol shows a blue shift of the main-chain onset absorption (λ_{onset} = 381 nm) relative to that of poly(**4**) in DMF (λ_{onset} = 438 nm), indicating a shorter main-chain conjugation in methanol. On the basis of the differential extinction coefficients between **4** and poly(**4**), curve e in Figure 4 was drawn to illustrate the main-chain absorption of poly(**4**) in DMF, which is centered at around 333 nm. Although such an absorption wavelength is significantly blue-shifted relative to that (λ_{max} = 390 nm) of the optically active poly(*N*-propargylamide) in chloroform reported by Masuda et al.[27] and was ascribed to a random-coil main-chain conformation,[28] the CD spectrum of poly(**4**) in DMF shows a negative Cotton effect ($[\theta] = -1.7 \times 10^4$ deg cm^2 dmol^{-1}) with molar ellipticity comparable to that of the helical poly(*N*-propargylamide)[27] in the main-chain absorption range, confirming the single-handed helical structure of the polymer. In contrast, monomer **4** shows no obvious CD signals in the spectral range investigated. In comparison with poly(**4**) in DMF, poly(**2**) in chloroform and poly(**4**) in methanol showed weaker and blue-shifted CD signals in the main-chain absorption range,

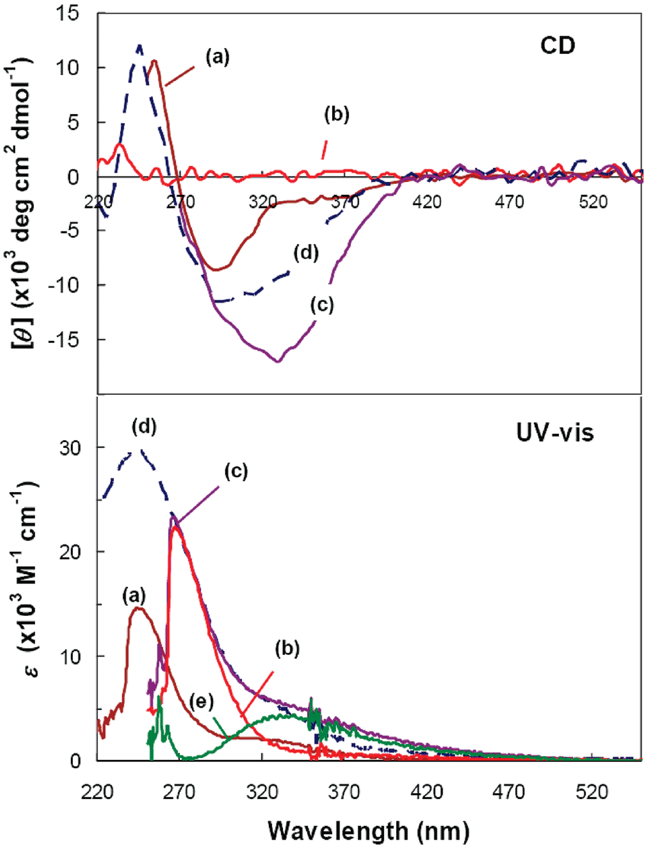

Figure 4. UV–vis and CD spectra of poly(**2**) in chloroform (a), **4** in DMF (b), poly(**4**) in DMF (c), and poly(**4**) in methanol (d). The main-chain absorption of poly(**4**) (e) is also shown by subtracting the extinction coefficient (ε) of poly(**4**) by the ε of **4**.

which is consistent with their relatively smaller ORs and can be attributed to different main-chain conformations.

Redox-Based UV–vis and CD Spectroscopies. The redox properties of viologen-containing poly(**4**) and **4** were studied in a DMF solution by CV using tetrabutylammonium perchlorate as the supporting electrolyte. As shown in Figure 5, **4** shows two major redox processes at $E_{1/2} = -0.36$ and -0.75 V, corresponding to the single-electron reduction processes of viologen from the double cationic (V^{2+}) state to the radical-cation (or violene, $V^{\bullet+}$) state and from the violene state to the neutral semiquinone (V) state, respectively. In contrast, poly(**4**) exhibits three one-electron redox patterns with $E_{1/2} = -0.35$, -0.76, and -0.89 V. Such a redox pattern is similar to those of double viologen-containing cyclic compounds investigated by us[16] and others[29] and can be attributed to short-range through-space electrostatic interactions between viologen groups. Masuda et al.[30] proposed two possible ways of intramolecular hydrogen bonding in single-handed helical poly(*N*-propargylamide), where hydrogen bonding forms between amide units from the *n*th to the ($n+2$)th or from the *n*th to the ($n+3$)th repeat units. By taking either of the proposed structures, an interchromophoric distance of around 4 Å can be estimated for viologens in the side chains of poly(**4**). Such a close distance of viologens is desirable in yielding large chiroptical properties according to the previous modeling results[15] and Kirkwood's coupled oscillator model.[31]

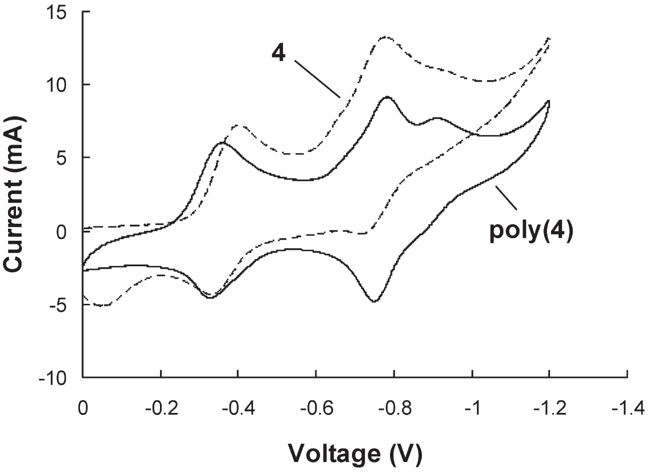

Figure 5. Cyclic voltammograms of **4** and poly(**4**) in a 0.1 M Bu$_4$NClO$_4$/DMF solution with a scan speed of 100 mV/s: working electrode, glassy carbon; counter electrode, platinum wire; reference electrode, AgCl/Ag.

Different from the viologen-containing conjugated polymer previously studied,[21] poly(**4**) showed relatively good reversibility of CV measurement. The redox cycles can be scanned many times without seeing deterioration of the sample solution (e.g., precipitation). However, when the polymer solution in DMF was subjected to electrochemical reduction at −0.5 V for a long period of time (e.g., 1 h), a yellow viscous precipitate became observable on the electrode. Therefore, the redox-based UV–vis and CD spectroscopies were measured by the previously reported chemical reduction method using a tin-particle-attached platinum grid as the reducing medium.[17] Figure 6 shows the UV–vis and CD spectra of poly(**4**) in DMF before and after chemical reduction. No optical absorption or CD signal is discernible above 450 nm before reduction. However, after chemical reduction by immersion of a tin-particle-attached platinum grid in the polymer solution in DMF for 1 h, a new strong UV–vis absorption band centered at around 600 nm appeared, which was accompanied with a negative CD band ($[\theta] = -8.0 \times 10^3$ deg cm^2 dmol^{-1}) at around 530 nm. The rotatory strength of this new CD band is calculated to be 1.3×10^{-40} esu^2 cm^2 according to Moffitt and Moscowitz's equation[32] and should contribute nontrivially to the specific rotation of poly(**4**) at NIR wavelengths (e.g., −15° at 850 nm and −9° at 1000 nm). Because the absorption at around 600 nm is due to the reduction-generated $V^{\bullet+}$, the appearance of the CD signal in this absorption band indicates an asymmetric spatial arrangement of the viologen groups in poly(**4**) induced by the single-handed helical main-chain structure. In contrast, no CD signal was observed for **4** in the $V^{\bullet+}$ absorption region, although a similar drastic color change from light yellow to dark blue also took place upon chemical reduction.

Figure 6 also shows an increasing absorption at around 550 nm, attributable to the pimerization of viologens, with the lengthening of the reduction time. Since monomer **4** exhibited no such an absorption upon reduction, a close positioning of viologens in poly(**4**) due to intramolecular hydrogen bond between amide units is confirmed. However, since transition dipoles of viologens, which are collinear along the long axes of the viologens, tend to be parallel with each other upon pimerization, which is contradictory to the requirement for twisting angles (e.g., ca. 60°) in achieving large chiroptical properties, pimerization of viologens is expected to contribute negatively to the reduction-induced chiroptical properties.

Chiroptical Switching. Although a few examples of chiroptically switching polymers based on photoisomerization[33] and temperature and chemical sensitivities[25,26,34] have been

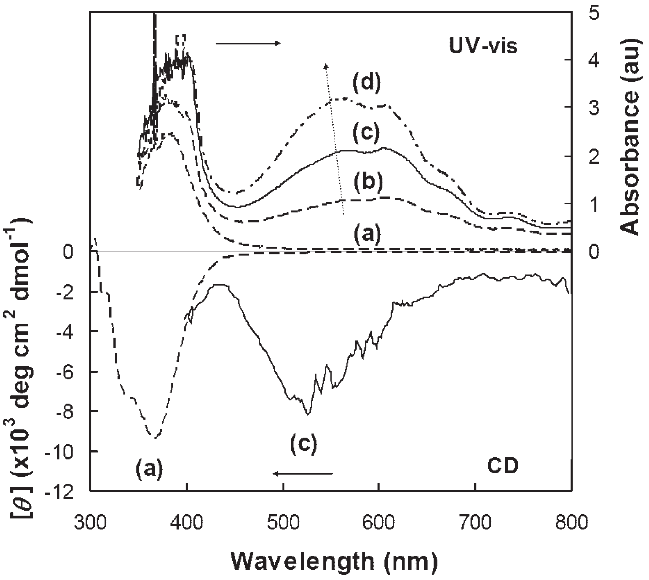

Figure 6. UV−vis (top) and CD (bottom) spectra of poly(**4**) in DMF ($c = 12.2$ mM) before (a) and after chemical reduction by immersion of a tin-particle-attached platinum grid into the solution for 20 min (b), 1 h (c), and 15 h (d).

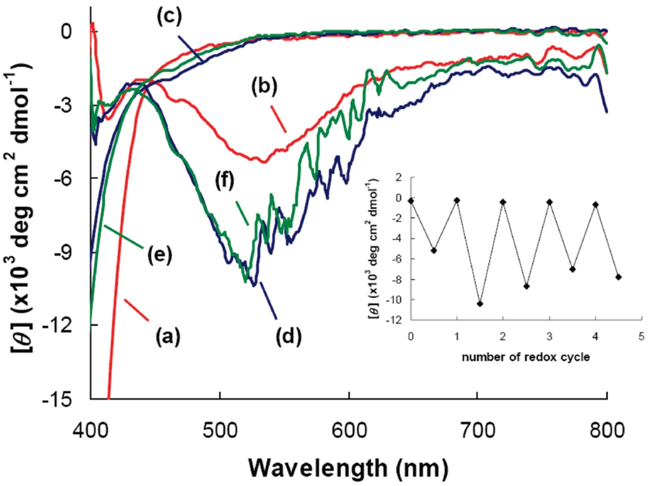

Figure 7. CD spectra of poly(**4**) in DMF ($c = 12.2$ mM) in the first three redox cycles: before reduction (a); first reduction by immersion of a tin-particle-attached platinum grid into a nitrogen-saturated polymer solution in DMF for 1 h (b); first oxidation done by shaking of the sample cell in air (c); second reduction (d); second oxidation (e); third reduction (f). The inset shows the switching of the CD signal at 526 nm.

reported, redox-driven chiroptically switching polymers are still rarely known.[35] Typically, redox-based chromism (e.g., electrochromism) is known to be capable of giving rise to large spectral changes with a maximal absorption wavelength readily tunable within the UV−vis−NIR spectral region (e.g., 200−2000 nm). Such a feature may be used to yield strong chiroptically switching properties once redox-active chromophores with good reversibility are properly positioned in the polymer. In our study, the chiroptically switching properties of poly(**4**) were examined in a DMF solution with repeated chemical reduction−oxidation cycles. The reduction was effected by immersion of a tin-particle-attached platinum grid into a nitrogen-saturated polymer solution in DMF for 1 h, and the oxidation of violenes was done by simple shaking of the sample cell in air. Figure 7 displays the CD spectra of the first three redox cycles and the switching CD signals at 526 nm. It can be seen that, upon reduction and oxidation, the CD signals corresponding to the violene absorption band can be generated and removed repeatedly. Although the intensities of the reduction-induced CD signals were not exactly the same for all of the redox processes, a good reversibility of the CD signals was observed after five reductions, as shown by the inset in Figure 7. No deterioration of the sample solution (e.g., precipitation) was observed during the study. The variation in the signal intensity can be attributed to the slow diffusion of violene polymers. Thin films of poly(**4**) on a conducting glass substrate (i.e., indium−tin oxide-coated glass) were also prepared and probed for their electrochromism and chiroptically switching properties. However, such an effort was not successful because of the weak color change at low reduction potentials (e.g., < −0.5 V) and the tendency of overreduction, as evidenced by the change of color to deep yellow, at high reduction potentials (e.g., > −0.6 V).

Conclusions

A redox-active single-handed helical polyacetylene bearing L-alanine and electrochromic viologen in the side chains was successfully prepared and carefully studied for the chiroptically switching properties. Because of the main-chain helical structure and the intramolecular hydrogen bonding, the viologen chromophores in the side chains were positioned closely and asymmetrically, which led the polymer to new distinctive CD signals at the long wavelengths (e.g., > 450 nm) upon reduction of cationic viologens to radical cations. The redox-driven CD switching was repeated five times without seeing deterioration of the sample solution, indicating a good redox reversibility of the polymer. Despite these, however, the switching magnitude of CD signals, e.g., between nearly 0 and −13 mdeg (or -1.0×10^4 deg cm^2 dmol^{-1}), which is comparable to that of previously studied viologen-containing polymer with axial main-chain chirality, is still not satisfactory. The diminished chiral perturbation effect of the helical main chain to the viologen groups due to strong intramolecular hydrogen bonding may hold one possible explanation for the moderate reduction-induced CD signals. Further optimization of the asymmetric spatial arrangement of chromophores is expected to lead to stronger chiroptically switching properties.

Acknowledgment. We are thankful for financial support from the National Natural Science Foundation of China (Grants 20774002 and 20834001) and SEM from the SRF for ROCS.

References and Notes

(1) (a) *Advances in Polymer Science: Polymers for Photonics Applications I*; Lee, K.-S., Ed.; Springer: Berlin, 2002; Vol. *158*. (b) *Advances in Polymer Science: Polymers for Photonics Applications II—Nonlinear Optical, Photorefractive and Two-Photon Absorption Polymers*; Lee, K.-S., Ed.; Springer: Berlin, 2003; Vol. *161*.
(2) (a) Schnabel, W. *Polymer and Light: Fundamentals and Technical Applications*; Wiley-VCH: Weinheim, Germany, 2007. (b) *Photonic Polymer Systems—Fundamentals, Methods, and Applications*; Wise, D. L., Wnek, G. E., Trantolo, D. J., Cooper, T. M., Gresser, J. D., Eds.; Marcel Dekker, Inc.: New York, 1998.
(3) Lippert, T. *Adv. Polym. Sci.* **2004**, *168*, 51.
(4) (a) Zhou, M. *Opt. Eng.* **2002**, *41*, 1631. (b) Ma, H.; Jen, A. K.-Y.; Dalton, L. R. *Adv. Mater.* **2002**, *14*, 1339. (c) Blythe, A. R.; Vinson, J. R. *Polym. Adv. Technol.* **2000**, *11*, 601.
(5) (a) Burland, D. M.; Miller, R. D.; Walsh, C. A. *Chem. Rev.* **1994**, *94*, 31. (b) Dalton, L. R.; Steier, W. H.; Robinson, B. H.; Zhang, C.; Ren, A.; Carner, S.; Chen, A.; Londergan, T.; Irwin, L.; Carlson, B.; Fifield, L.; Phelan, G.; Kincaid, C.; Amend, J.; Jen, A. *J. Mater. Chem.* **1999**, *9*, 1905.

(6) Grimsdale, A. C.; Chan, K. L.; Martin, R. E.; Jokisz, P. G.; Holmes, A. B. *Chem. Rev.* **2009**, *109*, 897.

(7) *Organic Photovoltaics—Mechanisms, Materials, and Devices*; Sun, S.-S., Sariciftci, N. S., Eds.; CRC Press: Boca Raton, FL, 2005.

(8) (a) Okamoto, Y.; Nakano, T. *Chem. Rev.* **1994**, *94*, 349. (b) Nolte, R. J. M. *Chem. Soc. Rev.* **1994**, *13*, 11. (c) Wulff, G. *Angew. Chem., Int. Ed. Engl.* **1995**, *34*, 1812. (d) Pu, L. *Chem. Rev.* **1998**, *98*, 2405.

(9) (a) Simpson, G. J. *ChemPhysChem* **2004**, *5*, 1301. (b) Verbiest, T.; Kauranen, M.; Persoons, A. *J. Mater. Chem.* **1999**, *9*, 2005. (c) Verbiest, T.; Elshocht, S. V.; Kauranen, M.; Hellemans, L.; Snauwaert, J.; Nuckolls, C.; Katz, T. J.; Persoons, A. *Science* **1998**, 913. (d) Ostroverkhov, Y.; Ostroverkhova, O.; Petschek, R. G.; Singer, K. D.; Sukhomlinova, L.; Twieg, R. J.; Wang, S.-X.; Chien, L. C. *Chem. Phys.* **2000**, *257*, 263.

(10) (a) Engheta, N.; Pelet, P. *Opt. Lett.* **1989**, *14*, 593. (b) Pelet, P.; Engheta, N. *J. Appl. Phys.* **1990**, *67*, 2742. (c) Herman, W. N.; Kim, Y.; Cao, W. L.; Goldhar, J.; Lee, C. H.; Green, M. M.; Jain, V.; Lee, M.-J. *J. Macromol. Sci.* **2003**, *A40*, 1369. (d) Herman, W. N. *J. Opt. Soc. Am. A* **2001**, *18*, 2806. (e) Kalvoda, L.; Polerecky, L. *Adv. Mater. Opt. Electron.* **1998**, *8*, 195.

(11) (a) Cheng, Q.; Cui, T. J.; Zhang, C. *Opt. Commun.* **2007**, *276*, 317. (b) Zhang, C.; Cui, T. J. *Opt. Commun.* **2007**, *280*, 359.

(12) (a) Feringa, B. L.; van Delden, R. A.; Koumura, N.; Geertseman, E. M. *Chem. Rev.* **2000**, *100*, 1789. (b) Hassey, R.; Swain, E. J.; Hammer, N. I.; Venkataraman, D.; Barnes, M. D. *Science* **2006**, *314*, 1437. (c) Wang, Z. Y.; Todd, E. K.; Meng, X. S.; Gao, J. P. *J. Am. Chem. Soc.* **2005**, *127*, 11552. (d) Zheng, J.; Qiao, W.; Wan, X.; Gao, J. P.; Wang, Z. Y. *Chem. Mater.* **2008**, *20*, 6163.

(13) (a) Gao, J. P.; Meng, X. S.; Bender, T. P.; Mackinnon, S.; Grand, V.; Wang, Z. Y. *Chem. Commun.* **1999**, 1281. (b) Martin, R. H. *Angew. Chem., Int. Ed. Engl.* **1974**, *13*, 649. (c) Katz, T. J.; Sudhakar, A.; Teasley, M. F.; Gilbert, A. M.; Geiger, W. E.; Robben, M. P.; Wuensch, M.; Ward, M. D. *J. Am. Chem. Soc.* **1993**, *115*, 3182.

(14) Nakano, T.; Okamoto, Y. *Chem. Rev.* **2001**, *101*, 4013.

(15) Deng, J.; Song, N.; Liu, W.; Zhou, Q.; Wang, Z. Y. *ChemPhysChem* **2008**, *9*, 1265.

(16) Deng, J.; Song, N.; Zhou, Q.; Su, Z. *Org. Lett.* **2007**, *9*, 5393.

(17) Deng, J.; Zhou, C.; Chen, C.; Song, N.; Su, Z. *Macromolecules* **2008**, *41*, 7805.

(18) (a) Green, M. M.; Jha, S. K. *Chirality* **1997**, *9*, 424. (b) Palmans, A. R. A.; Meijer, E. W. *Angew. Chem., Int. Ed.* **2007**, *46*, 8948. (c) Teramoto, A. *Prog. Polym. Sci.* **2001**, *26*, 667.

(19) Kikuchi, D.; Sakaguchi, S.; Ishii, Y. J. *J. Org. Chem.* **1998**, *63*, 6023.

(20) Tatsuya, M.; Nao, S.; Hiroshi, N. *J. Inclusion Phenom. Macrocycl. Chem.* **2006**, *56*, 141.

(21) Pepitone, M. F.; Jernigan, G. G.; Melinger, J. S.; Kim, O.-K. *Org. Lett.* **2007**, *9*, 801.

(22) Schrock, R. R.; Osborn, J. A. *Inorg. Chem.* **1970**, *9*, 2339.

(23) Gao, G.; Sanda, F.; Masuda, T. *Macromolecules* **2003**, *36*, 3932.

(24) (a) Alvaro, M.; Garcia, H.; Garcia, S.; Marquez, F.; Scaiano, J. C. *J. Phys. Chem. B* **1997**, *101*, 3043. (b) Ng, S. W.; Neoh, K. G.; Wong, Y. T.; Sampanthar, J. T.; Kang, E. T. *Langmuir* **2001**, *17*, 1766.

(25) Tabei, J.; Nomura, R.; Masuda, T. *Macromolecules* **2002**, *35*, 5405.

(26) Tabei, J.; Nomura, R.; Masuda, T. *Macromolecules* **2003**, *36*, 573.

(27) Nomura, R.; Tabei, J.; Masuda, T. *J. Am. Chem. Soc.* **2001**, *123*, 8430.

(28) Deng, J.; Tabei, J.; Shiotsuki, M.; Sanda, F.; Masuda, T. *Macromolecules* **2004**, *37*, 1891.

(29) (a) Anelli, P. L.; Ashton, P. R.; Ballardini, R.; Balzani, V.; Delgado, M.; Gandolfi, M. T.; Goodnow, T. T.; Kaifer, A. E.; Philp, D.; Pietraszkiewicz, M.; Prodi, L.; Reddington, M. V.; Slawin, A. M. Z.; Spencer, N.; Stoddart, J. F.; Vicent, C.; Williams, D. J. *J. Am. Chem. Soc.* **1992**, *114*, 193. (b) Geuder, V.; Hunig, S.; Suchy, A. *Tetrahedron* **1986**, *42*, 1665.

(30) Nomura, R.; Tabei, J.; Nishiura, S.; Masuda, T. *Macromolecules* **2003**, *36*, 561.

(31) (a) Kirkwood, J. G. *J. Chem. Phys.* **1937**, *5*, 479. (b) Moffitt, W. *J. Chem. Phys.* **1956**, *25*, 467. (c) Harada, N.; Chen, S.-M.; Nakanishi, L. K. *J. Am. Chem. Soc.* **1975**, *97*, 5345. (d) Eyring, H.; Liu, H.-C.; Caldwell, D. *Chem. Rev.* **1968**, *68*, 525.

(32) (a) Moscowitz, A. In *Optical Rotatory Dispersion*; Djerassi, C., Ed.; McGraw-Hill: New York, 1960; Vol. *12*.(b) Moffitt, W.; Moscowitz, A. *J. Chem. Phys.* **1959**, *30*, 648.

(33) (a) Muller, M.; Zentel, R. *Macromolecules* **1994**, *27*, 4404. (b) Kosaka, N.; Oda, T.; Hiyama, T.; Nozaki, K. *Macromolecules* **2004**, *37*, 3159. (c) Wang, C.; Zhu, L.; Xiang, J.; Yu, Y.; Zhang, D.; Shuai, Z.; Zhu, D. *J. Org. Chem.* **2007**, *72*, 4306. (d) Sanda, F.; Teraura, T.; Masuda, T. *J. Polym. Sci., Part A: Polym. Chem.* **2004**, *42*, 4641.

(34) Yashima, E.; Matsushima, T.; Okamoto, Y. *J. Am. Chem. Soc.* **1995**, *117*, 11596.

(35) (a) Redl, F. X.; Lutz, M.; Daub, J. *Chem.—Eur. J.* **2001**, *7*, 5350. (b) Plenio, H.; Hermann, J.; Sehring, A. *Chem.—Eur. J.* **2000**, *6*, 1820. (c) Goto, H.; Akagi, K. *Chem. Mater.* **2006**, *18*, 255.